Biochimica et Biophysica Acta 1853 (2015) 2173–2182

Contents lists available at ScienceDirect

Biochimica et Biophysica Acta

journal homepage: www.elsevier.com/locate/bbamcr

A novel chimeric aequorin fused with caveolin-1 reveals a sphingosine kinase 1-regulated Ca^{2+} microdomain in the caveolar compartment☆

Ilari Pulli [a,1], Tomas Blom [b,1], Christoffer Löf [c], Melissa Magnusson [a], Alessandro Rimessi [d], Paolo Pinton [d], Kid Törnquist [a,e,*]

[a] Åbo Akademi University, Tykistökatu 6A, 20520 Turku, Finland
[b] University Of Helsinki, 00014 Helsinki, Finland
[c] University Of Turku, Department of Physiology, Institute of Biomedicine, Kiinamyllynkatu 10, 20520 Turku, Finland
[d] University of Ferrara, Dept. of Morphology, Surgery and Experimental Medicine, Section of Pathology, Oncology and Experimental Biology, Laboratory for Technologies of Advanced Therapies (LTTA), 44121 Ferrara, Italy
[e] Minerva Foundation Institute For Medical Research, Biomedicum Helsinki, 00270 Helsinki, Finland

ARTICLE INFO

Article history:
Received 12 December 2014
Received in revised form 13 March 2015
Accepted 7 April 2015
Available online 16 April 2015

Keywords:
Caveolin-1
Aequorin
Sphingosine kinase 1
Sphingosine-1-phosphate
Calcium
Plasma membrane

ABSTRACT

Caveolae are plasma membrane invaginations enriched in sterols and sphingolipids. Sphingosine kinase 1 (SK1) is an oncogenic protein that converts sphingosine to sphingosine 1-phosphate (S1P), which is a messenger molecule involved in calcium signaling. Caveolae contain calcium responsive proteins, but the effects of SK1 or S1P on caveolar calcium signaling have not been investigated. We generated a Caveolin-1–Aequorin fusion protein (Cav1–Aeq) that can be employed for monitoring the local calcium concentration at the caveolae ($[Ca^{2+}]$cav). In HeLa cells, Cav1–Aeq reported different $[Ca^{2+}]$ as compared to the plasma membrane $[Ca^{2+}]$ in general (reported by SNAP25–Aeq) or as compared to the cytosolic $[Ca^{2+}]$ (reported by cyt-Aeq). The Ca^{2+} signals detected by Cav1–Aeq were significantly attenuated when the caveolar structures were disrupted by methyl-β-cyclodextrin, suggesting that the caveolae are specific targets for Ca^{2+} signaling. HeLa cells overexpressing SK1 showed increased $[Ca^{2+}]$cav during histamine-induced Ca^{2+} mobilization in the absence of extracellular Ca^{2+} as well as during receptor-operated Ca^{2+} entry (ROCE). The SK1-induced increase in $[Ca^{2+}]$cav during ROCE was reverted by S1P receptor antagonists. In accordance, pharmacologic inhibition of SK1 reduced the $[Ca^{2+}]$cav during ROCE. S1P treatment stimulated the $[Ca^{2+}]$cav upon ROCE. The Ca^{2+} responses at the plasma membrane in general were not affected by SK1 expression. In summary, our results show that SK1/S1P-signaling regulates Ca^{2+} signals at the caveolae. This article is part of a Special Issue entitled: 13th European Symposium on Calcium.

1. Introduction

Sphingosine kinase 1 (SK1) is an oncogenic protein that converts sphingosine to the lipid messenger molecule sphingosine-1-phosphate (S1P). Sphingosine and its metabolic precursor ceramide are considered to be pro-apoptotic lipids whereas S1P is involved in promoting cell survival. SK1/S1P signaling acts through direct intracellular mechanisms as well as through extracellular stimulation of specific G-protein coupled S1P receptors (S1PR1-5), some of which are known to couple to phospholipase C (PLC) [1,2]. Activation of PLC results in the hydrolysis of phosphatidylinositol 4,5-bisphosphate (PIP2) into two central Ca^{2+} signaling molecules, diacylglycerol (DAG) and inositol 1,4,5-trisphosphate (IP3).

Members of the transient receptor potential canonical channels (TRPC1-7) are activated upon DAG-binding [3], thus facilitating receptor-operated Ca^{2+} entry (ROCE) and S1P has been shown to be involved in this process [3,4]. In accordance, S1P treatment activates TRPC2 in rat thyroid FRTL-5 cells [5]. IP3 is a major regulator of the intracellular endoplasmic reticulum (ER) Ca^{2+} store and acts by ligating the IP3 receptor (IP3R) Ca^{2+} channels in the ER membrane [6]. There is also evidence for S1P to directly mediate the release of Ca^{2+} from the intracellular stores [7]. However, the role of SK1 and S1P in regulating Ca^{2+} signaling in specific cellular sub-compartments is poorly characterized.

Since the development of organelle-specific Ca^{2+} reporters, it has become increasingly evident that highly localized Ca^{2+} signals regulate various cell physiological phenomena. For instance, recent reports have highlighted the importance of mitochondrial Ca^{2+} handling in multiple (patho)physiological situations, and the long-sought molecular identity of the mitochondrial Ca^{2+} uniporter (MCU) complex is now emerging [8–11]. Also, the importance of the interplay between the major Ca^{2+} store, the endoplasmic reticulum (ER), and the mitochondria is being characterized [12,13]. Furthermore, the lysosomal compartments are involved in cellular Ca^{2+} handling [14].

☆ This article is part of a Special Issue entitled: 13th European Symposium on Calcium.
* Corresponding author. Tel.: +358 50 5855262.
E-mail address: ktornqvi@abo.fi (K. Törnquist).
[1] Authors contributed equally.

http://dx.doi.org/10.1016/j.bbamcr.2015.04.005
0167-4889/

In addition to the Ca^{2+} domains in membrane enclosed organelles, local micro domains of cytosolic Ca^{2+} play a role in cell physiological events. Such Ca^{2+} micro domains may for instance arise near channels and pumps involved in Ca^{2+} handling near the plasma membrane (PM) or the ER [15,16]. Many components of the cellular Ca^{2+} handling reside in the PM. These include the plasma membrane Ca^{2+} ATPases (PMCAs), ion channels of the transient receptor potential (TRP) family, and the Orai channels with functions ranging from maintaining the Ca^{2+} homeostasis to regulation of cell proliferation and migration. PM and ER have been shown to interact to regulate Ca^{2+} fluxes. For instance, the stromal interaction molecules (STIMs) that reside in the ER and sense the luminal Ca^{2+} concentrations of the organelle can couple to the Orai and TRP canonical (TRPC) channels to activate store-operated calcium entry (SOCE) [17,18].

To organize cellular signaling, the lipid and protein composition of the PM is compartmentalized through cytoskeletal and integral membrane protein scaffolding [19]. Caveolae are invaginated cholesterol-rich compartments of the PM which are involved in facilitating and organizing cellular signals. Caveolin proteins (caveolin1–3) are the main structural components of caveolae, caveolin-1 being the most abundantly expressed isoform in most tissues. Caveolae have numerous proposed functions including the regulation of local Ca^{2+} signaling as well as contact coordination at the PM, ER and mitochondrial interfaces. Multiple molecules that are related to Ca^{2+} signaling have been shown to localize to caveolae, including G-protein coupled receptors (GPCRs), receptor tyrosine kinases (RTKs), ion channels (e.g. TRPC1 and 4) as well as PIP2, PLC and IP3R. Also scaffolding functions for caveolin-1 mediating the activity of TRPC1 upon SOCE have been proposed [20–22].

Depending on the cellular context, SK1 may translocate to the caveolin-1 enriched domains in PM upon activation [23]. This PM translocation of SK1 is in part mediated by Ca^{2+} [24] and may facilitate S1P secretion to the cell exterior, leading to autocrine S1P signaling [5,24–26]. Since caveolae are versatile Ca^{2+} signaling domains with implicated functions for all of the major cellular Ca^{2+} handling mechanisms (i.e. ER Ca^{2+}-release through the IP3R channels and Ca^{2+}-uptake through ROCE and SOCE), we wanted to investigate whether SK1-mediated signaling would act locally at the caveolae to coordinate some of these central Ca^{2+} signaling events.

Experimental methods for measuring Ca^{2+} at the caveolae are relatively limited. Ca^{2+} signaling molecules interacting with caveolae-associated structures are to some extent characterized, but experimental data for specific caveolar Ca^{2+} fluxes is scarce. To our knowledge, two approaches to investigate Ca^{2+} signaling related to caveolae have been reported. By employing targeted fluorescent Ca^{2+} reporters and FRET, Isshiki et al. [27,28] have shown that caveolae are the preferred plasma membrane domains for SOCE, and that the internalized caveolin-enclosed vesicles may act as sealed compartments that are able to release Ca^{2+} in an IP3R-dependent manner.

Here, we characterize a novel chimeric Ca^{2+} reporter protein comprising of the Asp119Ala-mutated aequorin [29] and caveolin-1 (designated here as Cav1–Aeq) that specifically reports Ca^{2+} signals from a caveolar microdomain. These Ca^{2+} signals are registered at the cytoplasmic subcellular domain near to the caveolae and are distinct from the Ca^{2+} signals from the overall near PM Ca^{2+} compartment. By employing this approach, we show novel roles for the oncogenic protein SK1 in controlling the caveolar Ca^{2+} microdomain upon IP3R stimulation, ROCE and SOCE.

2. Materials and methods

2.1. Cell culture, transduction and transfection

HeLa cells were cultured in DMEM (#D5546, Sigma-Aldrich) supplemented with 10% FBS, 1% penicillin–streptomycin and 1% L-glutamine (Life Technologies) at 37 °C and 5% CO_2. The ML1 thyroid cancer cells that were used in a supplementary experiment were grown in the same medium as described here for HeLa cells. To overexpress SK1, we used a previously described lentiviral expression vector [5]. Transduction with the SK1 overexpression vector was performed by incubating the cells with polybrene (8 mg/ml) along with the viral particles at multiplicity of infection 10 for 6 h. Control cells were created by mock-vector transduction. The lentiviral particles for SK1 shRNA (sc-156038-V), as well as the control vectors (sc-108080), were acquired from Santa Cruz Biotechnology and the cells were transduced by incubating the cells for 12 h with polybrene (8 mg/ml) along with the lentiviral particles at multiplicity of infection 30. After 24 h the cells were subjected to continuous selection with 0.5 mg/ml puromycin (Life Technologies). Plasmid transfection mixtures were prepared by using TurboFect transfection reagent (#R0531, Thermo Scientific), OptiMEM media (#31985-070, Life Technologies) and 1 μg/ml plasmid (final concentration). The transfections were conducted in the same cell culture conditions as described above.

2.2. Construction of the caveolin-1–aequorin plasmid

For measurements in the caveolar compartment we created a plasmid chimera with the sequences for caveolin-1 and the previously described Asp119Ala-mutated aequorin (mut-Aeq) [29]. Among other targeting sequences (see Materials and methods, Section 2.6 for additional references), this mut-Aeq has been previously characterized for the plasma membrane targeting SNAP25–Aeq chimera [29]. The Cav1–Aeq was generated by amplifying Cav-1 using the primers (5-CGGGGT ACCATGTCTGGGGGAAATAC-3; forward, 5-GGCGAATTCTATTTCTTTCT GCAAGTTGAT-3; reverse). The PCR fragment was subcloned into a pSC-A vector. The fragment coding Cav-1 was excised by KpnI and EcoRI digestion, and the fragment encoding Cav-1 was ligated into pcDNA3 to generate pcDNA3-Cav1. The mut-Aeq fragment was cut from a pSC-A plasmid using EcoRI, and ligated into the pcDNA3-Cav1, to generate the pcDNA3-Cav1–Aeq encoding a chimeric protein with the N-terminus of mut-Aeq fused to the C-terminus of caveolin-1. N-terminal modifications to the mut-Aeq have been shown not to affect the luminescence production of the chimeric proteins [30].

2.3. Separation of detergent resistant membrane fractions on Optiprep gradient

All steps were performed at +4 °C. Cells were washed 2× in PBS, harvested and pelleted by centrifugation for 5 min at 2500 rpm. The cells were homogenized in 250 μl TNE buffer (25 mM Tris–HCl pH 7.5, 150 mM NaCl, 5 mM EDTA, 0.1% Triton-X 100, 10% sucrose, 1 mM DTT and protease inhibitor cocktail). The lysate was blended with 480 μl 60% Optiprep and mixed. The lysate was transferred to an ultracentrifuge tube, and TNE buffer with decreasing percent Optiprep were layered on top. The samples were centrifuged for 4 h, 40,000 rpm using a Beckman Coulter centrifuge with a SW 60Ti rotor after which the fractions were collected in Eppendorf tubes.

2.4. Western blot

For western blotting, the cells were grown to 70% confluence, followed by three washes with phosphate buffered saline (PBS) on ice. The cells were then lysed by addition of 3x Laemmli sample buffer (LSB), where after the lysates were boiled for 5 min. Then, the proteins were subjected to SDS-PAGE and transferred to a nitrocellulose membrane. The membranes were then blocked with 5% milk in TBS (Tris-buffered saline, 150 mM NaCl, 20 mM Tris base, pH 7.5) with 0.1% Tween 20 (Sigma-Aldrich) and incubated overnight with the desired primary antibody at +4 °C. The primary antibodies were diluted 1:1000 in PBS containing 0.5% bovine serum albumin (BSA). Then, the membranes were washed and incubated with the secondary, horseradish peroxidase (HRP) conjugated antibodies (1:3000 dilution in

TBST + 5% milk). The proteins were then detected by chemiluminescence using Western Lightning Plus-ECL substrate (Perkin Elmer). The sphingosine kinase 1 antibody was from Cell Signaling and the HSC70 antibody was from Enzo life sciences. The caveolin-1 antibody was from Santa Cruz and the anti-HA antibody from Sigma-Aldrich.

2.5. Immunocytochemistry and microscopy

For immunocytochemistry, the cells were grown on poly-L-lysine coated coverslips and, when targeted fluorescent plasmids were used, transfected with the desired plasmid constructs. Then, the cells were washed three times with PBS and fixed with 4% paraformaldehyde in PBS for 15 min, followed by three washes and a 5-minute treatment with 1% Triton-X in PBS. Next, the cells were treated with 1% BSA in PBS for 1 h followed by three washes in PBS. Then, the cells were treated overnight at +4 °C with the desired primary antibody. After this, the cells were washed, treated with the secondary antibodies and mounted using Mowiol mounting medium. The primary antibodies used were caveolin-1 (#sc-894, Santa Cruz) and anti-HA (#H9658, Sigma-Aldrich). The AlexaFluor secondary antibodies were from Life Technologies. The ER-GFP was described before in [31] and the plasmids encoding RFP and EGFP tagged CAV1 were from Addgene (plasmids #14434 and #27704, deposited by Ari Helenius, described in [32]). TIRF microscopy was performed with a Nikon Eclipse Ti-E microscope using a 100×/1.49 NA oil immersion objective. ER-GFP and Cav1-RFP were excited by the 488 nm and 561 nm laser lines, respectively. The calculated imaging depth was ~100 nm, and the microscope was controlled with NIS-Elements Advanced Research 3.1 (Nikon). Widefield microscopy was done using the same microscope with epifluorescence settings and a 40×/0.75 objective. Confocal microscopy was done on a Leica TCS SP2 attached to a DM RXA2 microscope using a 63×/0.90 NA water immersion objective.

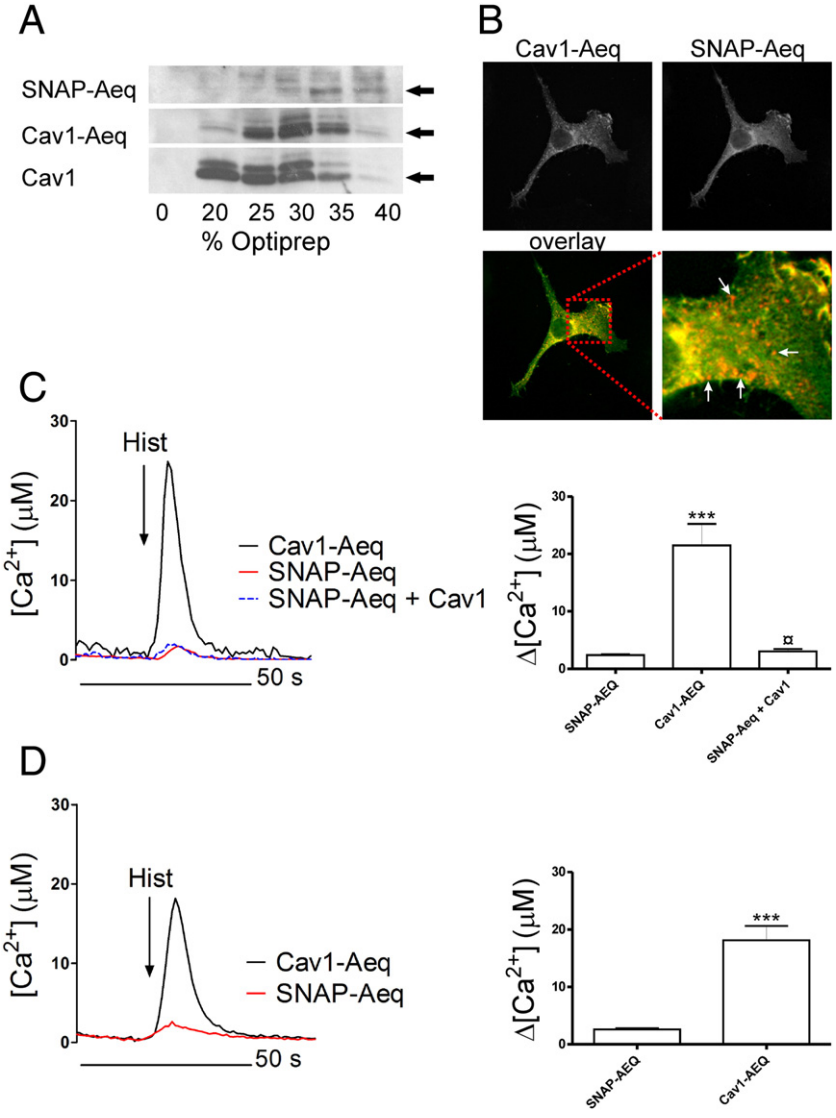

Fig. 1. Caveolae sense Ca^{2+}-signals differently from the plasma membrane. (A) HeLa cells overexpressing Caveolin-1–Aequorin (Cav1–Aeq) and SNAP25–Aequorin (SNAP–Aeq) were harvested and detergent resistant and soluble fractions were separated on an Optiprep gradient by ultracentrifugation. The gradient fractions were collected and the detergent resistance of the indicated proteins was addressed by western blotting. (B) Confocal images showing the distribution of Cav1–Aeq (pseudo color red, indicated by white arrows in the magnification) versus SNAP–AEQ (pseudo color green). (C) HeLa cells transfected with Cav1–Aeq, SNAP–Aeq or SNAP–Aeq + Cav1–EGFP were stimulated with 100 μM histamine in Ca^{2+}-free conditions. Representative traces are shown. The bar diagrams show the average change in $[Ca^{2+}]$. The error bar depicts S.E.M., n = 4–20, ***P < 0.001 (SNAP–AEQ compared to Cav1–AEQ), ¤P < 0.01 (Cav1–AEQ compared to SNAP–Aeq + Cav1) (D) HeLa cells were stimulated with 100 μM histamine in Ca^{2+}-containing (1 mM) conditions. Representative traces are shown. The bar diagrams show the average change in $[Ca^{2+}]$. The error bar depicts S.E.M., n = 12–13, ***P < 0.001.

2.6. Aequorin-based Ca^{2+} measurements

Measurements of subplasmalemmal [Ca^{2+}] and cytosolic [Ca^{2+}] were conducted by employing the SNAP25-fused aequorin or the non-targeted aequorin (cyt-Aeq), respectively, as described in [29]. Cav1–Aeq was employed for the measurements of [Ca^{2+}]cav. The general experimental setup was as described in [33]. Briefly, one hundred thousand cells per well were seeded on 12-well plates containing poly-L-lysine (Sigma-Aldrich) coated round 13 mm coverslips. The following day, the cells were transfected with the desired plasmid constructs as described in Section 2.1. Twenty-four hours after transfection the cells were washed three times with Ca^{2+} free HEPES-buffered saline solution (HBSS: 118 mM NaCl, 4.6 mM KCl, 10 mM glucose and 20 mM HEPES) supplemented with 150 μM EGTA. Thereafter, the cells were incubated for 1 h in HBSS containing 150 μM EGTA and 5 μM wild-type coelenterazine (#s053, Synchem). To record the luminescence the cells were transferred to a purpose-built chamber and perfused with the desired solutions at 37 °C. The sampling rate of the luminescence recordings was set to one measurement per second. The intracellular Ca^{2+} stores were replenished by incubating the cells in HBSS containing 1 mM Ca^{2+} for 2–3 min before starting the experimental treatments. The maximal luminescence of each sample was obtained by permeating the cells with 100 μM digitonin (Sigma-Aldrich) in HBSS containing 10 mM Ca^{2+}. The results were then calibrated using the calibration values for Asp119Ala-mutated aequorins as described in [29,34–39]. Histamine was from Sigma-Aldrich, the sphingosine kinase inhibitor

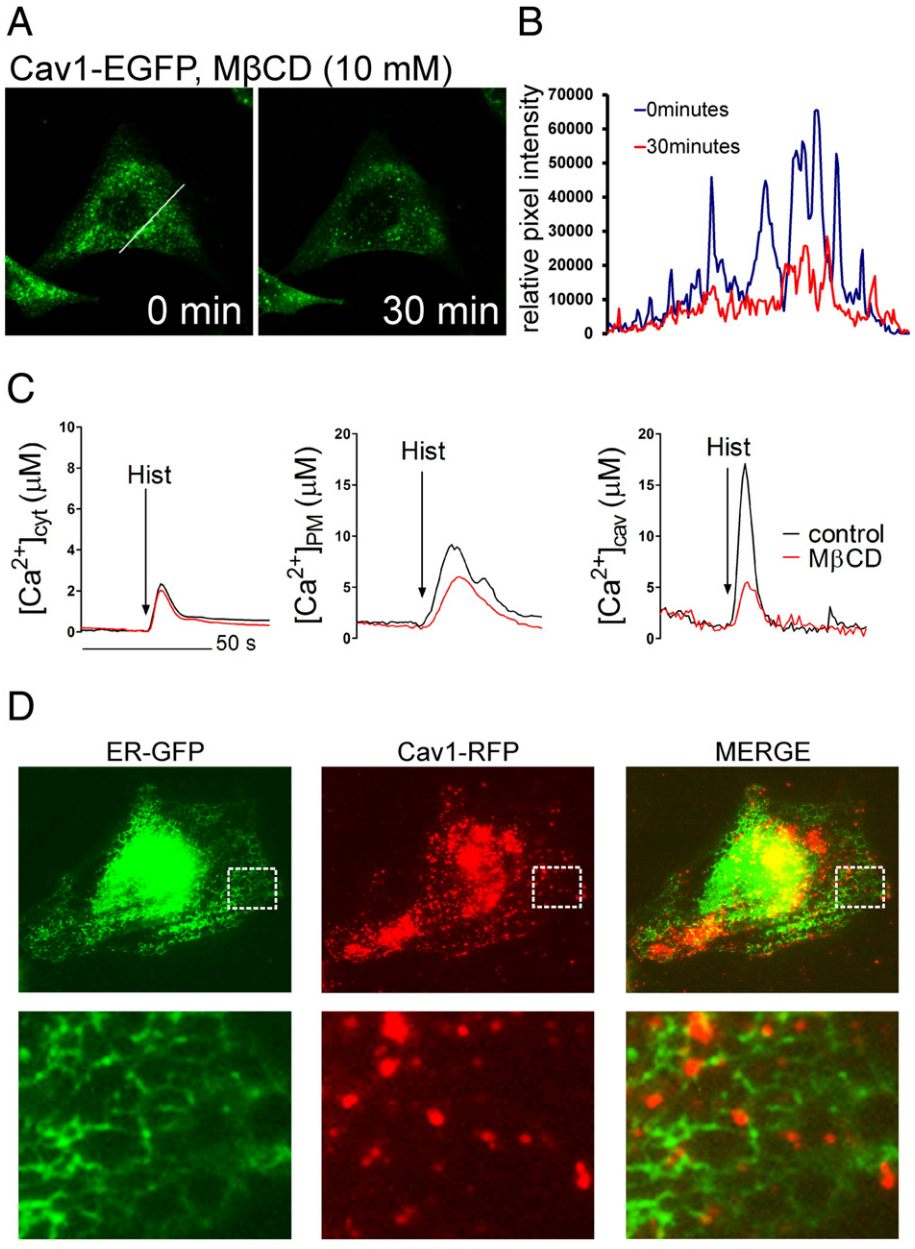

Fig. 2. Disrupting caveolae by depleting plasma membrane cholesterol leads to an attenuation of the Ca^{2+}-signal sensed by Cav1–Aeq. (A) Hela cells overexpressing Cav1–EGFP were imaged by confocal microscopy before and after treatment with 10 mM MβCD for 30 min. (B) Cav1–EGFP intensity along the line displayed in (A), before and after MβCD treatment. (C) HeLa cells transfected with cytosolic Aeq (cyt-Aeq), SNAP25–Aeq or cav1–Aeq were treated with or without 10 mM MβCD for 30 min, and Ca^{2+} transients at the bulk cytosol, at the plasma membrane (PM) or at the caveolae, respectively, were measured upon stimulation with 100 μM Histamine in the presence of 1 mM Ca^{2+}. Representative traces of 4–10 separate experiments are shown. Please note the different scale in cytosolic measurements. (D) TIRF microscopy pictures of HeLa cells expressing Cav1–RFP and ER-GFP. The lower panels are magnifications from the area within the rectangles (dotted line) in the upper panels.

was from Calbiochem (#567731), JTE013 was from Tocris (#2391) and VPC23019 was from Avanti Polar Lipids (#857360P). Sphingosine 1-phosphate (S1P) was from Enzo Life Sciences. JTE013 and sphingosine kinase inhibitor were dissolved in DMSO. VPC23019 was dissolved according to the compound datasheet (95 parts of 3% fatty acid free bovine serum albumin and 5 parts acidified DMSO). S1P was dissolved in HBSS buffer containing 4 mg/mL fatty acid free bovine serum albumin. The solvents served as controls.

2.7. Ca^{2+} measurements using Fura-2 AM

For Ca^{2+} experiments where Fura-2 AM (Life Technologies) was employed, the cells were grown on 25 mm poly-L-lysine coated coverslips, washed three times in HBSS and incubated for 30 min with 2 μM Fura-2 AM at room temperature (RT). Then the cells were washed and incubated for 15 min at RT. The coverslips were then transferred to a Sykes-Moore gasket which was mounted on a custom-made holder for perfusions. The excitation filters were set to 340 and 380 nanometers (nm), respectively, and the emission was recorded at 510 nm. The filters were controlled by a Lambda 10-2 device (Sutter Instruments, USA) and the excitation light was produced by an XBO 75 W/2 xenon lamp. To collect the images, we used an inverted Zeiss Axiovert 35 microscope with a Hamamatsu ORCA2 camera. The recordings were operated with an Axon Imaging Workbench software (version 6.0, Axon Instruments, USA). The recording frequency was set to one image per second and the fluorescence ratio (F_{340}/F_{380}) at each measured time point was used to evaluate the changes in cytosolic Ca^{2+}.

2.8. Statistics

Statistical analysis of the data was conducted by unpaired Student's t-test when two variables were compared or by One-Way Anova with Tukey's post-hoc test when three or more variables were compared. P-values below 0.05 were considered as statistically significant. The results are shown with S.E.M.

3. Results

3.1. Caveolin-1-aequorin chimera reports Ca^{2+} signals specifically from the caveolar microdomain

Caveolae are rich in sphingolipids and cholesterol and form distinct "raft-like" domains in the PM. The caveolae are associated with proteins central to Ca^{2+} signaling cascades [40–43] and thus likely play an important role in coordinating Ca^{2+} signaling events. In order to study Ca^{2+} signaling in caveolae, we generated a novel chimeric protein of caveolin-1 and aequorin (Cav1–Aeq). First, we validated the correct subcellular localization of Cav1–Aeq and its usefulness as reporter of caveolar Ca^{2+} signals in HeLa cells.

Cav1–Aeq partitioned similarly to endogenous caveolin-1 to the detergent resistant membrane fractions on an Optiprep gradient, while the general PM reporter SNAP–Aeq was found mainly in the soluble fraction (Fig. 1A). Immunofluorescence staining showed that Cav1–Aeq separated into small domains on the cell surface (Fig. 1B) in a similar fashion as Cav1-RFP (Supplementary Fig. 1), while SNAP–Aeq was distributed uniformly on the PM (Fig. 1B), as reported previously [34]. The caveolar Ca^{2+} responses ($[Ca^{2+}]$cav) reported by Cav1–Aeq differed substantially from the Ca^{2+} responses in the PM ($[Ca^{2+}]$PM) reported by SNAP25–aequorin chimera (SNAP–Aeq). When intracellular Ca^{2+} stores were mobilized by histamine stimulation in Ca^{2+} free medium, the peak of $[Ca^{2+}]$cav was higher than $[Ca^{2+}]$PM. Importantly, $[Ca^{2+}]$PM was not affected by caveolin-1 expression (Fig. 1C). Also, $[Ca^{2+}]$cav was higher than $[Ca^{2+}]$PM upon histamine stimulation in a Ca^{2+}-containing buffer (Fig. 1D).

To further verify that Cav1–Aeq reports Ca^{2+} transients in caveolar domains, we disrupted the caveolar structures by removing PM cholesterol using methyl-β-cyclodextrin (MβCD) (Fig. 2A, B). The MβCD treatment did not affect the cytosolic Ca^{2+} response upon histamine treatment suggesting that MβCD does not interfere with the mobilization of intracellular Ca^{2+} stores (Fig. 2C, left panel, the average $\Delta[Ca^{2+}] \pm$ S.E.M. were 2.24 ± 0.14 (control) and 1.84 ± 0.11 (MβCD), $P > 0.05$). The $[Ca^{2+}]$PM was reduced by approximately 40% (Fig. 2C, middle panel, the average $\Delta[Ca^{2+}] \pm$ S.E.M. were 8.5 ± 0.6 (control) and 5.1 ± 0.27 (MβCD), $P < 0.01$) which may be due to the cholesterol-dependence of SNAP-25 for effective PM localization [44]. However, the Ca^{2+} transient reported by the dispersed Cav1–Aeq in MβCD treated cells was blunted by approximately 80% (Fig. 2C, right panel, the average $\Delta[Ca^{2+}] \pm$ S.E.M. were 14.3 ± 1.9 (control) and 2.7 ± 1.1 (MβCD), $P < 0.001$), indicating that the Ca^{2+} signaling is

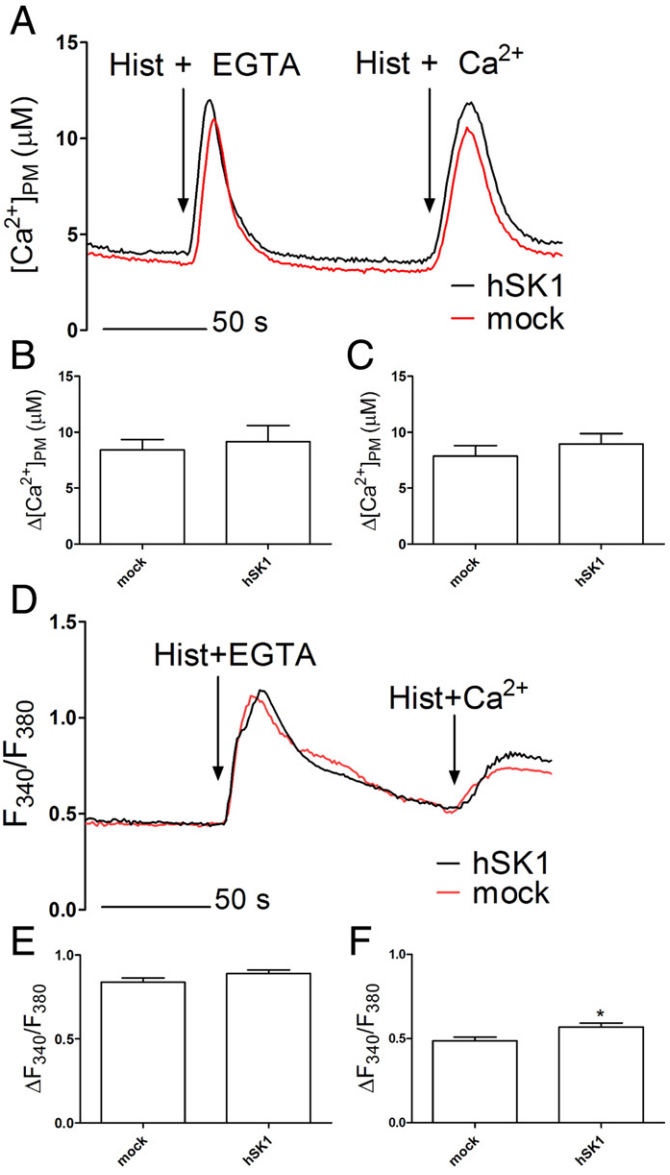

Fig. 3. The effect of SK1-overexpression on $[Ca^{2+}]$ at the plasma membrane as reported by SNAP25–aequorin (SNAP–Aeq) and in the cytosol as reported by Fura-2 AM. (A) Representative traces showing $[Ca^{2+}]$PM during histamine (100 μM) stimulation in presence of EGTA (150 μM), and Ca^{2+} (1 mM) re-addition (ROCE). Bar diagrams show the mean with S.E.M. indicating the change in $[Ca^{2+}]$PM during histamine-stimulation (B), and during Ca^{2+} re-addition (C), n = 5. (D) Average traces showing the Fura-2 AM fluorescence ratio (F_{340}/F_{380}) upon the same experimental conditions as in (A). The bar diagrams show the mean with S.E.M. indicating the change in the fluorescence ratio ($\Delta F_{340}/F_{380}$) during histamine stimulation in the presence of EGTA (E) and during Ca^{2+} re-addition (F), n = 6, *$P < 0.05$.

directed towards properly assembled caveolae and not the caveolin-1 protein by itself.

In HeLa cells, histamine is known to mobilize Ca^{2+} from the ER by activating the PLC/IP3/IP3R pathway [45]. Interestingly, TIRF microscopy showed that ER tubules in close proximity to the PM tend to associate with caveolae (Fig. 2D). These results establish that Cav1–Aeq is a useful probe for measuring caveolar Ca^{2+} transients. Moreover, the histamine-induced Ca^{2+} mobilization seems to be concentrated in the vicinity of caveolae.

3.2. Sphingosine kinase 1 regulates [Ca^{2+}] specifically at caveolar microdomains

As caveolae are enriched in sphingomyelin [46] and have been reported to associate with receptors for the sphingomyelin metabolite S1P [47], we next utilized the Cav1–Aeq probe to test whether sphingosine kinase 1/S1P induced Ca^{2+} signaling is integrated at caveolae.

To investigate the importance of SK1 in HeLa cells, we created cell lines where SK1 is either overexpressed (hSK1 cells) or downregulated (shSK1 cells) with the respective control cell lines (mock and shC cells). The SK1 protein levels were approximately 4-fold higher in the hSK1 as compared to the mock control cells (Supplementary Fig. 2). Since caveolae are rich in sphingolipids and caveolae have shown to contain multiple components of the Ca^{2+} signaling machinery, we wanted to investigate whether SK1 could be involved in Ca^{2+} signaling locally at the caveolar sub-compartment of the PM. To test this hypothesis, we employed Cav1–Aeq reporter and compared the caveolar Ca^{2+} signals to the overall PM Ca^{2+} signals by utilizing the previously characterized SNAP–Aeq [29].

First, we performed experiments where the cells were stimulated with 100 μM histamine in presence of 150 μM EGTA, which was followed by Ca^{2+} 1 mM re-addition (induction of ROCE). During the both phases of this experiment, the [Ca^{2+}]PM response remained unchanged upon SK1 overexpression, compared with control cells (Fig. 3A, B, C). The cytosolic Ca^{2+} responses ([Ca^{2+}]$_i$), as reported by the Ca^{2+} indicator Fura-2 AM, were unaffected by SK1 overexpression during 100 μM histamine stimulation in the presence of 150 μM EGTA (Fig. 3D & E) and slightly but significantly increased upon ROCE (Fig. 3D & F). However, we found that [Ca^{2+}]cav was increased by SK1 overexpression during both phases of the experiment, as compared with control cells. Furthermore, the SK1-induced increase in [Ca^{2+}]cav during ROCE was sensitive to the S1PR inhibitors JTE013 (10 μM) and VPC23019 (1 μM) (Fig. 4). Interestingly, stable SK1 overexpression in ML1 thyroid cancer cells showed increased [Ca^{2+}]cav during 40 μM ATP stimulation in the presence of 150 μM EGTA but not during the 1 mM Ca^{2+} re-addition (Supplementary Fig. 3). Also, please note the effect of the control solutions (see Materials and methods, Section 2.6) on [Ca^{2+}]cav as evidenced by comparison of Fig. 4 and Supplementary Fig. 4.

To study the possibility that extracellular S1P regulates the caveolar Ca^{2+} microdomain, we acutely treated HeLa cells with 700 nM S1P and conducted caveolar Ca^{2+} measurements with the same experimental protocol as in Fig. 3. Interestingly, we found that acute S1P treatment was without an effect during the histamine-induced Ca^{2+}-release from the intracellular Ca^{2+} stores (Fig. 5A), whereas upon ROCE the uptake of Ca^{2+} via caveolae was augmented by S1P (Fig. 5A & B). We next asked whether pharmacological inhibition of SK1 might have an effect. For this purpose, we treated HeLa cells with a SK inhibitor (SKi; 10 μM for 1 h), followed by the same experimental procedures as in Fig. 3. SKi, or the vehicle DMSO, were present throughout the whole experiment. This experiment showed that SKi blocked the Ca^{2+}-uptake during ROCE (Fig. 5C & D), whereas Ca^{2+}-release upon histamine

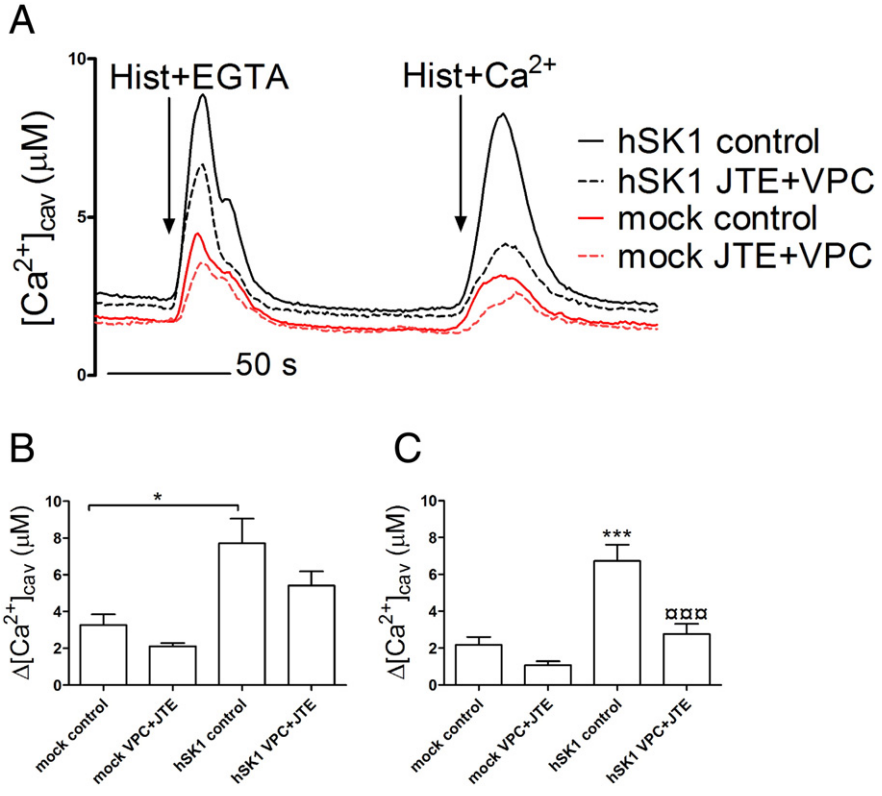

Fig. 4. Overexpression of SK1 induces an increase in [Ca^{2+}]cav during histamine-stimulated release of endoplasmic Ca^{2+}, as well as during receptor-operated Ca^{2+} entry (ROCE). The cells were pretreated for 1 h with either 1 μM VPC and 10 μM JTE in combination, or with the control solutions. Following the pre-incubation, the compounds were present throughout the experiments. A) Representative traces of experiments showing [Ca^{2+}]cav during histamine (100 μM) stimulation in presence of EGTA (150 μM), and Ca^{2+} (1 mM) re-addition (ROCE). B) Quantification of the change in [Ca^{2+}] at the caveolae during histamine-induced Ca^{2+} mobilization in the absence of extracellular Ca^{2+}. C) Quantification of the change in [Ca^{2+}]cav during Ca^{2+} re-addition in the presence of histamine. The bar diagrams show the mean with S.E.M., n = 7–10, *P < 0.05, ***P < 0.001 (mock control vs hSK1 control), ¤¤¤P < 0.001 (hSK1 control vs hSK1 VPC + JTE).

stimulation in extracellular Ca^{2+} free condition was not significantly changed (Fig. 5C). The $[Ca^{2+}]$PM was unaffected by S1P treatment whereas the SKi treatment diminished the Ca^{2+} during ROCE (Supplementary Fig. 5).

To indirectly assess whether SK1 induces the increase in $[Ca^{2+}]$cav through increased physical interactions between the ER and caveolae, we performed an experiment where the ER Ca^{2+} is passively released by ionomycin (5 μM) treatment in the absence of extracellular Ca^{2+}. In this case, SK1 did not affect $[Ca^{2+}]$cav (Fig. 6) indicating that the physical ER-caveolae contact sites remain unaltered upon SK1 overexpression.

Sphingosine, the substrate for SK1, is known to block the interactions between STIM1 and Orai1 at the cell membrane, thus attenuating store-operated Ca^{2+} entry in the cells [48]. Therefore, we performed thapsigargin (TG, 1 μM) induced store-operated Ca^{2+} entry (SOCE) experiments. Overexpression of SK1 did not affect the $[Ca^{2+}]$ at the caveolae or at the PM during SOCE (Fig. 7), whereas cells with SK1 downregulation (Supplementary Fig. 2) displayed slightly reduced $[Ca^{2+}]$cav upon SOCE, leaving the $[Ca^{2+}]$PM fluxes unchanged (Fig. 7). Cellular sphingosine has been shown to accumulate upon SK1 downregulation [49]. Therefore, we find it possible that sphingosine levels are increased in our shSK1 HeLa cells, which might facilitate the sphingosine-induced inhibition of SOC channels, and reduced SOCE at the caveolae.

4. Discussion

Caveolin-1 expression has been associated to regulation of cancer progression in a multifaceted and context-dependent manner. Caveolin-1 has both anti-tumorigenic as well as cancer-promoting qualities [20,50,51]. In this work, we describe a novel probe for investigating Ca^{2+} signaling at the cytoplasmic face of the caveolae. Further, we establish that with our approach it is possible to detect truly distinguishable Ca^{2+} microdomains at the caveolae that functionally differ from the overall PM Ca^{2+} domain (Figs. 1 & 2).

By comparing overall PM Ca^{2+} levels to those reported by Cav1–Aeq we show that specific Ca^{2+} signaling events are taking place locally at the caveolae upon altered expression levels of the oncogenic protein SK1. These findings represent interesting examples for the local Ca^{2+} microdomain signaling that has been proposed to be coordinated at the caveolae or directly controlled via scaffolding functions of caveolin-1.

Deranged regulation of Ca^{2+} handling is an emerging concept in cancer biology affecting many aspects of cancer cell physiology such as proliferation, cellular migration and deregulated apoptotic pathways. These physiological processes are in part regulated by intricate Ca^{2+} signaling events that are controlled by a multitude of specialized Ca^{2+} channels, Ca^{2+} pumps and exchangers, Ca^{2+} binding proteins, as well as cellular organelles and compartments [52,53]. In this context, our findings on the SK1-mediated caveolar Ca^{2+} microdomain may have several functional implications.

As we demonstrate here, overexpression of SK1 induces an increase in $[Ca^{2+}]$cav upon the histamine-stimulated, IP3-receptor mediated Ca^{2+}-release when extracellular Ca^{2+} is chelated, while the $[Ca^{2+}]$PM remains unaltered. This effect of SK1 was not blocked by S1PR1-3 antagonism indicating that autocrine S1P signaling might not play a major role here.

However, IP3Rs and ER may be found in close association to caveolae [21], and S1P has been shown to directly release Ca^{2+} from the ER [54]. Also, SK1 is known to be activated and translocated in a Ca^{2+}-dependent manner [24] and Serine225 phosphorylation of SK1 guides the activated kinase to caveolin-1 enriched lipid raft domains of the PM [23]. Thus, it may be feasible to motivate this SK1-induced increase in $[Ca^{2+}]$cav by a Ca^{2+}-activated local S1P production. Further, local Ca^{2+}-induced Ca^{2+} release (CICR) [6] might play a role in amplifying the SK1-induced $[Ca^{2+}]$cav.

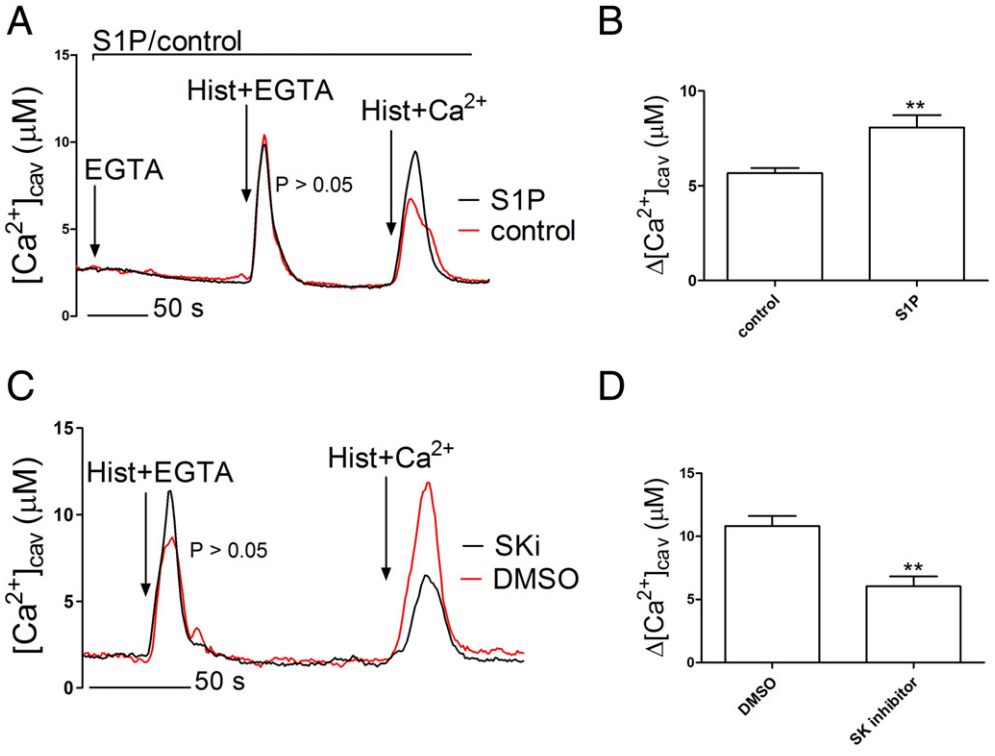

Fig. 5. Sphingosine 1-phosphate (S1P) treatment increases Ca^{2+} at the caveolar compartment during receptor-operated Ca^{2+} entry whereas SK inhibitor (SKi) blocks ROCE. A) Representative traces of an experiment where the cells were acutely treated with 700 nM S1P as indicated in the figure, followed by consecutive perfusions with histamine (150 μM) in the presence of 150 μM EGTA and 1 mM Ca^{2+}, respectively. B) Quantification of the Ca^{2+} addition in (A), showing the mean with S.E.M., $^{**}p < 0.01$, $n = 5$. C) Representative traces from an experiment where the cells were pre-treated for 60 min with 10 μM SKi and stimulated with histamine in the presence of 150 μM EGTA, followed by 1 mM Ca^{2+} re-addition. SKi or DMSO was present throughout the whole experiment. D) Quantification of the Ca^{2+} re-addition in (C) showing the mean with S.E.M., $^{**}p < 0.01$, $n = 5$ for DMSO, $n = 7$ for SK inhibitor.

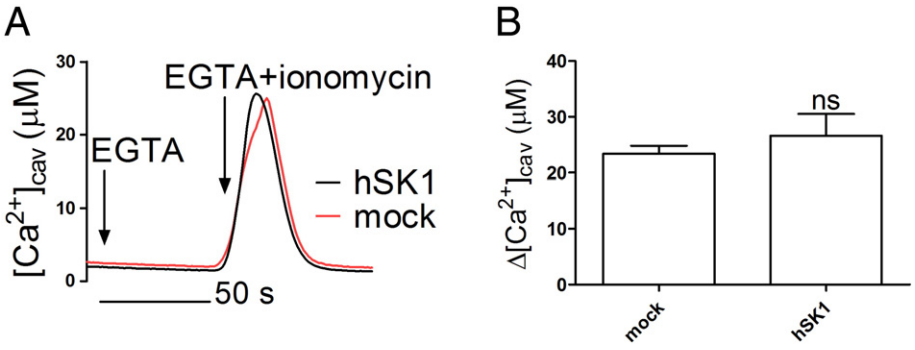

Fig. 6. Ionomycin treatment in presence of EGTA does not show a SK1-induced caveolar microdomain. The cells were perfused with HBSS containing 150 μM EGTA followed by perfusion with EGTA and 5 μM ionomycin. Representative traces (A) and bar diagrams indicating the mean with S.E.M. (B) are shown, n = 3, ns = not significant.

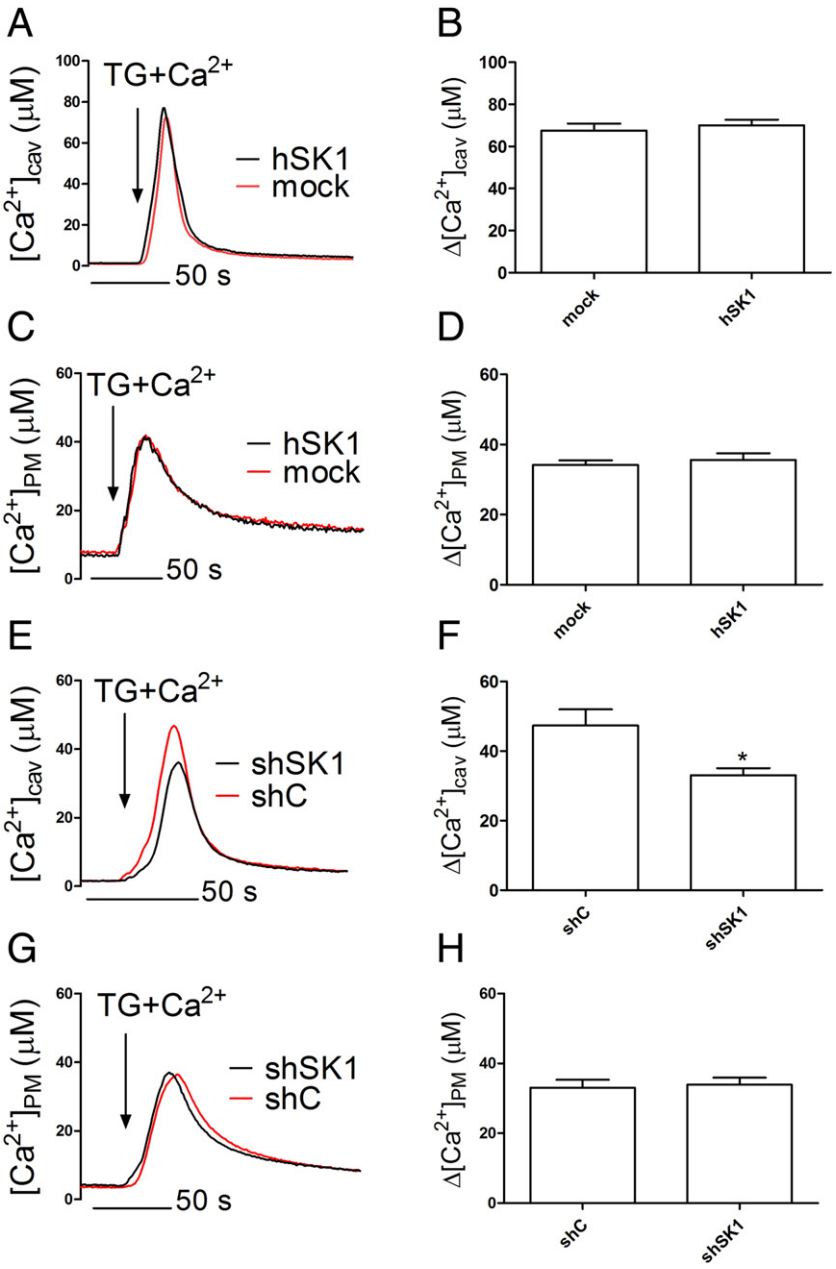

Fig. 7. Store-operated Ca^{2+} entry (SOCE) at the caveolae and at the plasma membrane upon SK1 overexpression and downregulation, respectively. The cells were pre-treated with 1 μM thapsigargin (TG) in HBSS containing EGTA (150 μM) for 4 min. Then, the cells were perfused with 1 mM Ca^{2+} in the presence of 1 μM TG. SOCE was not affected by SK1 overexpression at the caveolae (A, B) nor at the PM (C, D), whereas knock-down of SK1 resulted in diminished SOCE specifically at the caveolae (E, F) but not at the overall PM (G, H). The bar diagrams indicate the means with S.E.M., n = 3–6, *P < 0.05.

Also, we show that caveolar ROCE is increased upon SK1 overexpression and this effect of SK1 is reversed by antagonizing the S1PR1-3. Further, we demonstrate that S1P treatment mimics SK1 overexpression by increasing $[Ca^{2+}]$cav upon ROCE, whereas SK1 inhibition attenuates ROCE in the caveolar domain. It has been shown that S1PR1 is localized to the caveolar fraction [47] and as noted above, SK1 translocates to caveolin-1 enriched lipid rafts upon activation. The increased ROCE through caveolae could thus be explained by autocrine S1P signaling, where S1P receptor activation leads to generation of DAG to promote ROC channel opening [55] upon histamine stimulation locally at the caveolae.

Interestingly, SK1 seems to affect Ca^{2+} mobilization and ROCE via two partially independent signaling pathways. The SK1 effect on ROCE is highly dependent on S1PR1-3 and can be reproduced by acute addition of S1P and antagonized by SK1-inhibition. In contrast, the effect of SK1 on histamine-induced Ca^{2+} mobilization is largely independent of S1PR1-3 and is not significantly affected by short term treatment with S1P or by acute inhibition of SK1. These results suggest that SK1 affects Ca^{2+} mobilization by a process requiring long term adaptation of the cells, while ROCE can be regulated on short notice.

Further, our results may have implications for the oncogenic actions of SK1. As SK1 activity and translocation are controlled by Ca^{2+}, it is possible that aberrant SK1 overexpression could lead to deranged amplification of other cellular Ca^{2+} signals through over-activated autocrine or intracellular S1P signaling. This would, in turn, lead to aberrant activation of ROCE or increased local Ca^{2+} release from the intracellular stores. SK1 induced increase in $[Ca^{2+}]$cav, during both IP3-receptor stimulation and ROCE, might then have importance for oncogenic processes such as deregulated cytoskeletal and focal adhesion assembly, leading to altered migratory capacity of the cells [53].

Taken together, we describe here a novel tool for Ca^{2+} measurement that reports Ca^{2+} concentrations from the caveolar domain of the PM. By employing this method, we show for the first time the importance of SK1 for regulating local Ca^{2+} signaling at this PM microdomain.

Supplementary data to this article can be found online at http://dx.doi.org/10.1016/j.bbamcr.2015.04.005.

Disclosure of conflicts of interest

The authors declare that there are no conflicts of interest.

Acknowledgment

This work was supported by grants to I.P. from Tor, Joe och Pentti Borgs Minnesfond, Oscar Öflunds stiftelse and Svenska Kulturfonden, and by grants to T.B. from Academy of Finland (grant number 266092), Stiftelsens för Åbo Akademi Forskningsinstitut, Liv och Hälsa and Magnus Ehrnrooths sfiftelse as well as by funding to K.T. from Sigrid Juselius Foundation and the Centre of Excellence in Cell Stress and Molecular Ageing (Åbo Akademi University).

References

[1] S.M. Pitson, Regulation of sphingosine kinase and sphingolipid signaling, Trends Biochem. Sci. 36 (2011) 97–107.
[2] N.J. Pyne, F. Tonelli, K.G. Lim, J.S. Long, J. Edwards, S. Pyne, Sphingosine 1-phosphate signalling in cancer, Biochem. Soc. Trans. 40 (2012) 94–100.
[3] S. Crousillac, J. Colonna, E. McMains, J.S. Dewey, E. Gleason, Sphingosine-1-phosphate elicits receptor-dependent calcium signaling in retinal amacrine cells, J. Neurophysiol. 102 (2009) 3295–3309.
[4] E. Palazzo, F. Rossi, V. de Novellis, S. Maione, Endogenous modulators of TRP channels, Curr. Top. Med. Chem. 13 (2013) 398–407.
[5] D. Gratschev, C. Lof, J. Heikkila, A. Bjorkbom, P. Sukumaran, A. Hinkkanen, J.P. Slotte, K. Tornquist, Sphingosine kinase as a regulator of calcium entry through autocrine sphingosine 1-phosphate signaling in thyroid FRTL-5 cells, Endocrinology 150 (2009) 5125–5134.
[6] J.K. Foskett, C. White, K.H. Cheung, D.O. Mak, Inositol trisphosphate receptor Ca^{2+} release channels, Physiol. Rev. 87 (2007) 593–658.
[7] D. Meyer zu Heringdorf, K. Liliom, M. Schaefer, K. Danneberg, J.H. Jaggar, G. Tigyi, K.H. Jakobs, Photolysis of intracellular caged sphingosine-1-phosphate causes Ca^{2+} mobilization independently of G-protein-coupled receptors, FEBS Lett. 554 (2003) 443–449.
[8] S. Marchi, P. Pinton, The mitochondrial calcium uniporter complex: molecular components, structure and physiopathological implications, J. Physiol. 592 (2014) 829–839.
[9] D. De Stefani, A. Raffaello, E. Teardo, I. Szabo, R. Rizzuto, A forty-kilodalton protein of the inner membrane is the mitochondrial calcium uniporter, Nature 476 (2011) 336–340.
[10] G. Csordas, T. Golenar, E.L. Seifert, K.J. Kamer, Y. Sancak, F. Perocchi, C. Moffat, D. Weaver, S. de la Fuente Perez, R. Bogorad, V. Koteliansky, J. Adijanto, V.K. Mootha, G. Hajnoczky, MICU1 controls both the threshold and cooperative activation of the mitochondrial Ca(2)(+) uniporter, Cell Metab. 17 (2013) 976–987.
[11] K. Mallilankaraman, C. Cardenas, P.J. Doonan, H.C. Chandramoorthy, K.M. Irrinki, T. Golenar, G. Csordas, P. Madireddi, J. Yang, M. Muller, R. Miller, J.E. Kolesar, J. Molgo, B. Kaufman, G. Hajnoczky, J.K. Foskett, M. Madesh, MCUR1 is an essential component of mitochondrial Ca^{2+} uptake that regulates cellular metabolism, Nat. Cell Biol. 14 (2012) 1336–1343.
[12] B. Kornmann, The molecular hug between the ER and the mitochondria, Curr. Opin. Cell Biol. 25 (2013) 443–448.
[13] G. Hajnoczky, D. Booth, G. Csordas, V. Debattisti, T. Golenar, S. Naghdi, N. Niknejad, M. Paillard, E.L. Seifert, D. Weaver, Reliance of ER-mitochondrial calcium signaling on mitochondrial EF-hand Ca^{2+} binding proteins: Miros, MICUs, LETM1 and solute carriers, Curr. Opin. Cell Biol. 29 (2014) 133–141.
[14] A.J. Morgan, F.M. Platt, E. Lloyd-Evans, A. Galione, Molecular mechanisms of endolysosomal Ca^{2+} signalling in health and disease, Biochem. J. 439 (2011) 349–374.
[15] M.J. Berridge, Calcium microdomains: organization and function, Cell Calcium 40 (2006) 405–412.
[16] R. Rizzuto, T. Pozzan, Microdomains of intracellular Ca^{2+}: molecular determinants and functional consequences, Physiol. Rev. 86 (2006) 369–408.
[17] M.J. Berridge, M.D. Bootman, H.L. Roderick, Calcium signalling: dynamics, homeostasis and remodelling, Nat. Rev. Mol. Cell Biol. 4 (2003) 517–529.
[18] J. Soboloff, B.S. Rothberg, M. Madesh, D.L. Gill, STIM proteins: dynamic calcium signal transducers, Nat. Rev. Mol. Cell Biol. 13 (2012) 549–565.
[19] B.P. Head, H.H. Patel, P.A. Insel, Interaction of membrane/lipid rafts with the cytoskeleton: impact on signaling and function: membrane/lipid rafts, mediators of cytoskeletal arrangement and cell signaling, Biochim. Biophys. Acta 1838 (2014) 532–545.
[20] R.G. Parton, M.A. del Pozo, Caveolae as plasma membrane sensors, protectors and organizers, Nat. Rev. Mol. Cell Biol. 14 (2013) 98–112.
[21] B. Pani, B.B. Singh, Lipid rafts/caveolae as microdomains of calcium signaling, Cell Calcium 45 (2009) 625–633.
[22] B. Pani, H.L. Ong, S.C. Brazer, X. Liu, K. Rauser, B.B. Singh, I.S. Ambudkar, Activation of TRPC1 by STIM1 in ER-PM microdomains involves release of the channel from its scaffold caveolin-1, Proc. Natl. Acad. Sci. U. S. A. 106 (2009) 20087–20092.
[23] J.A. Hengst, J.M. Guilford, T.E. Fox, X. Wang, E.J. Conroy, J.K. Yun, Sphingosine kinase 1 localized to the plasma membrane lipid raft microdomain overcomes serum deprivation induced growth inhibition, Arch. Biochem. Biophys. 492 (2009) 62–73.
[24] K.E. Jarman, P.A. Moretti, J.R. Zebol, S.M. Pitson, Translocation of sphingosine kinase 1 to the plasma membrane is mediated by calcium- and integrin-binding protein 1, J. Biol. Chem. 285 (2010) 483–492.
[25] D. Siow, B. Wattenberg, The compartmentalization and translocation of the sphingosine kinases: mechanisms and functions in cell signaling and sphingolipid metabolism, Crit. Rev. Biochem. Mol. Biol. 46 (2011) 365–375.
[26] T. Blom, N. Bergelin, A. Meinander, C. Lof, J.P. Slotte, J.E. Eriksson, K. Tornquist, An autocrine sphingosine-1-phosphate signaling loop enhances NF-kappaB-activation and survival, BMC Cell Biol. 11 (2010) (45-2121-11-45).
[27] M. Isshiki, Y.S. Ying, T. Fujita, R.G. Anderson, A molecular sensor detects signal transduction from caveolae in living cells, J. Biol. Chem. 277 (2002) 43389–43398.
[28] M. Isshiki, M. Nishimoto, R. Mizuno, T. Fujita, FRET-based sensor analysis reveals caveolae are spatially distinct Ca^{2+} stores in endothelial cells, Cell Calcium 54 (2013) 395–403.
[29] M. Bonora, C. Giorgi, A. Bononi, S. Marchi, S. Patergnani, A. Rimessi, R. Rizzuto, P. Pinton, Subcellular calcium measurements in mammalian cells using jellyfish photoprotein aequorin-based probes, Nat. Protoc. 8 (2013) 2105–2118.
[30] J.M. Kendall, G. Sala-Newby, V. Ghalaut, R.L. Dormer, A.K. Campbell, Engineering the CA(2+)-activated photoprotein aequorin with reduced affinity for calcium, Biochem. Biophys. Res. Commun. 187 (1992) 1091–1097.
[31] R. Rizzuto, P. Pinton, W. Carrington, F.S. Fay, K.E. Fogarty, L.M. Lifshitz, R.A. Tuft, T. Pozzan, Close contacts with the endoplasmic reticulum as determinants of mitochondrial Ca^{2+} responses, Science 280 (1998) 1763–1766.
[32] A. Hayer, M. Stoeber, C. Bissig, A. Helenius, Biogenesis of caveolae: stepwise assembly of large caveolin and cavin complexes, Traffic 11 (2010) 361–382.
[33] A. Hyrskyluoto, I. Pulli, K. Tornqvist, T.H. Ho, L. Korhonen, D. Lindholm, Sigma-1 receptor agonist PRE084 is protective against mutant huntingtin-induced cell degeneration: involvement of calpastatin and the NF-kappaB pathway, Cell. Death Dis. 4 (2013) e646.
[34] R. Marsault, M. Murgia, T. Pozzan, R. Rizzuto, Domains of high Ca^{2+} beneath the plasma membrane of living A7r5 cells, EMBO J. 16 (1997) 1575–1581.
[35] M. Montero, J. Alvarez, W.J. Scheenen, R. Rizzuto, J. Meldolesi, T. Pozzan, Ca^{2+} homeostasis in the endoplasmic reticulum: coexistence of high and low $[Ca^{2+}]$ subcompartments in intact HeLa cells, J. Cell Biol. 139 (1997) 601–611.
[36] P. Pinton, T. Pozzan, R. Rizzuto, The Golgi apparatus is an inositol 1,4,5-trisphosphate-sensitive Ca^{2+} store, with functional properties distinct from those of the endoplasmic reticulum, EMBO J. 17 (1998) 5298–5308.

[37] K.J. Mitchell, P. Pinton, A. Varadi, C. Tacchetti, E.K. Ainscow, T. Pozzan, R. Rizzuto, G.A. Rutter, Dense core secretory vesicles revealed as a dynamic Ca(2+) store in neuroendocrine cells with a vesicle-associated membrane protein aequorin chimaera, J. Cell Biol. 155 (2001) 41–51.
[38] F.M. Lasorsa, P. Pinton, L. Palmieri, P. Scarcia, H. Rottensteiner, R. Rizzuto, F. Palmieri, Peroxisomes as novel players in cell calcium homeostasis, J. Biol. Chem. 283 (2008) 15300–15308.
[39] S. Marchi, L. Lupini, S. Patergnani, A. Rimessi, S. Missiroli, M. Bonora, A. Bononi, F. Corra, C. Giorgi, E. De Marchi, F. Poletti, R. Gafa, G. Lanza, M. Negrini, R. Rizzuto, P. Pinton, Downregulation of the mitochondrial calcium uniporter by cancer-related miR-25, Curr. Biol. 23 (2013) 58–63.
[40] D. Marques-da-Silva, C. Gutierrez-Merino, Caveolin-rich lipid rafts of the plasma membrane of mature cerebellar granule neurons are microcompartments for calcium/reactive oxygen and nitrogen species cross-talk signaling, Cell Calcium 56 (2014) 108–123.
[41] T. Fujimoto, Calcium pump of the plasma membrane is localized in caveolae, J. Cell Biol. 120 (1993) 1147–1157.
[42] T. Fujimoto, S. Nakade, A. Miyawaki, K. Mikoshiba, K. Ogawa, Localization of inositol 1,4,5-trisphosphate receptor-like protein in plasmalemmal caveolae, J. Cell Biol. 119 (1992) 1507–1513.
[43] M. Isshiki, J. Ando, K. Yamamoto, T. Fujita, Y. Ying, R.G. Anderson, Sites of Ca(2+) wave initiation move with caveolae to the trailing edge of migrating cells, J. Cell Sci. 115 (2002) 475–484.
[44] J. Vikman, J. Jimenez-Feltstrom, P. Nyman, J. Thelin, L. Eliasson, Insulin secretion is highly sensitive to desorption of plasma membrane cholesterol, FASEB J. 23 (2009) 58–67.
[45] S. Ishida, T. Matsu-Ura, K. Fukami, T. Michikawa, K. Mikoshiba, Phospholipase C-beta1 and beta4 contribute to non-genetic cell-to-cell variability in histamine-induced calcium signals in HeLa cells, PLoS One 9 (2014) e86410.
[46] M. Taniguchi, T. Okazaki, The role of sphingomyelin and sphingomyelin synthases in cell death, proliferation and migration-from cell and animal models to human disorders, Biochim. Biophys. Acta 1841 (2014) 692–703.
[47] C.K. Means, S. Miyamoto, J. Chun, J.H. Brown, S1P1 receptor localization confers selectivity for Gi-mediated cAMP and contractile responses, J. Biol. Chem. 283 (2008) 11954–11963.
[48] N. Calloway, M. Vig, J.P. Kinet, D. Holowka, B. Baird, Molecular clustering of STIM1 with Orai1/CRACM1 at the plasma membrane depends dynamically on depletion of Ca^{2+} stores and on electrostatic interactions, Mol. Biol. Cell 20 (2009) 389–399.
[49] N. Kotelevets, D. Fabbro, A. Huwiler, U. Zangemeister-Wittke, Targeting sphingosine kinase 1 in carcinoma cells decreases proliferation and survival by compromising PKC activity and cytokinesis, PLoS One 7 (2012) e39209.
[50] A. Rimessi, S. Marchi, S. Patergnani, P. Pinton, H-Ras-driven tumoral maintenance is sustained through caveolin-1-dependent alterations in calcium signaling, Oncogene 33 (2014) 2329–2340.
[51] H. Yu, H. Shen, Y. Zhang, F. Zhong, Y. Liu, L. Qin, P. Yang, CAV1 promotes HCC cell progression and metastasis through Wnt/beta-catenin pathway, PLoS One 9 (2014) e106451.
[52] N. Prevarskaya, H. Ouadid-Ahidouch, R. Skryma, Y. Shuba, Remodelling of Ca^{2+} transport in cancer: how it contributes to cancer hallmarks? Philos. Trans. R. Soc. Lond. B Biol. Sci. 369 (2014) 20130097.
[53] N. Prevarskaya, R. Skryma, Y. Shuba, Calcium in tumour metastasis: new roles for known actors, Nat. Rev. Cancer 11 (2011) 609–618.
[54] G.M. Strub, M. Maceyka, N.C. Hait, S. Milstien, S. Spiegel, Extracellular and intracellular actions of sphingosine-1-phosphate, Adv. Exp. Med. Biol. 688 (2010) 141–155.
[55] D.J. Beech, Integration of transient receptor potential canonical channels with lipids, Acta Physiol. (Oxf.) 204 (2012) 227–237.